Synthesis and structures of $Cu^{I,II}$ complexes with a 2,2′-bipyridine derivative bearing a (+)-3-carene moiety*

T. E. Kokina,[a,b]★ L. A. Glinskaya,[a] D. A. Piryazev,[a] A. Yu. Baranov,[b,c] A. M. Agafontsev,[b,c] Yu. A. Eremina,[a,b] E. V. Vorontsova,[d] A. S. Bogomyakov,[e] D. Yu. Naumov,[a,b] A. V. Tkachev,[b,c] and S. V. Larionov[a,b]

[a]*Nikolaev Institute of Inorganic Chemistry, Siberian Branch of the Russian Academy of Sciences, 3 prosp. Akad. Lavrentieva, 630090 Novosibirsk, Russian Federation. Fax: +7 (383) 330 9489. E-mail: niic@niic.nsc.ru*

[b]*Novosibirsk State University, 2 ul. Pirogova, 630090 Novosibirsk, Russian Federation. Email: kokina@niic.nsc.ru*

[c]*N. N. Vorozhtsov Novosibirsk Institute of Organic Chemistry, Siberian Branch of the Russian Academy of Sciences, 9 prosp. Akad. Lavrentieva, 630090 Novosibirsk, Russian Federation*

[d]*Institute of Molecular Biology and Biophysics, 2/12 ul. Timakova, 630117 Novosibirsk, Russian Federation*

[e]*International Tomography Center, Siberian Branch of the Russian Academy of Sciences, 3a ul. Institutskaya, 630090 Novosibirsk, Russian Federation. Fax: +7 (383) 333 1399. E-mail: bus@tomo.nsc.ru*

The complex salt $\{[CuL_2][Cu_4I_6]\cdot MeCN\}_n$ (**1**) and the compound $[Cu_4L_3I_4]\cdot 3\ MeCN$ (**2**) (**L** is a chiral ligand bearing a natural monoterpene (+)-3-carene moiety) were synthesized. The crystal structures of compounds **1** and **2** were determined by X-ray diffraction. The structure of compound **1** consists of complex cations $[CuL_2]^{2+}$ (N_3O_2 polyhedron is a trigonal bipyramid) and Cu^I coordination polymers (CuI_4 polyhedron is a tetrahedron) as anions. The experimental magnetic moment μ_{eff} at 300 K is 1.90 μ_B, which is consistent with the X-ray diffraction data and the assumption that compound **1** is mixed-valence. The structure of compound **2** comprises a tetranuclear Cu^I complex, in which three Cu atoms are coordinated by two N atoms of the ligand **L** and two I atoms, and the fourth Cu atom is coordinated by four I atoms (coordination polyhedra are distorted tetrahedra). Compounds **L** and **2** were found to influence the viability of human laryngeal carcinoma cells (Hep2). The IC_{50} value for complex **2** (13.0±1.7 μ*M*) is substantially smaller than IC_{50} for compound **L** (30.5±0.5 μ*M*).

Key words: copper(I,II) complexes, chiral ligand, terpenes, iodide complex, crystal structure, coordination framework, cytotoxicity.

The synthesis and structure determination of metal complexes with chiral ligands have attracted considerable attention of researchers in the field of coordination chemistry. This interest is associated with the fact that the reactions of metal ions with chiral ligands can afford products with unique properties. Such complexes hold promise as chiral biologically active substances,[1] luminescent compounds,[2—5] single-molecule magnets,[6,7] and so on.

Among ligands used for the synthesis of chiral coordination compounds, optically active natural products, including natural terpene derivatives, are of particular interest. Terpenes, which serve as the starting compounds for the synthesis of this class of chiral ligands, are widespread in plants and have high enantiomeric purity. The largest number of coordination compounds synthesized to date contain chiral ligands based on such available terpenes as α-pinene, β-pinene, (+)-3-carene, and limonene.[1,8—12] Many of the synthesized complexes have unique physical properties. For example, luminescent chiral lanthanide complexes with *N*-heterocyclic ligands containing pinene moieties[2,13] or camphor moieties[5,14] were prepared. The synthesis of luminescent Zn^{II} and Cd^{II} complexes with this type of ligands was reported.[15—19]

The preparation of copper complexes with chiral terpene-containing ligands is an interesting task. First, Cu^{II} complexes, as well as Cu^I complexes with various organic ligands are extensively studied as promising therapeutic agents.[20—23] The cytotoxicity of metal complexes based on a number of chiral ligands was reported.[24] Biological

* Based on the materials of the XXVII International Chugaev Conference on Coordination Chemistry (October 2—6, 2017; Nizhny Novgorod, Russia).

Published in Russian in *Izvestiya Akademii Nauk. Seriya Khimicheskaya,* No. 7, pp. 1251—1260, July, 2018.

1066-5285/18/6707-1251 © 2018 Springer Science+Business Media, Inc.

activity of copper complexes with terpene derivatives as ligands is poorly known.[25—27] Second, considerable attention is paid to Cu^{I} complexes, particularly halide clusters, which can have promising photophysical properties.[8,29]

The goal of this work is to synthesize copper complexes with chiral *N*-[(1a*S*,3*S*,7b*R*)-1,1,3-trimethyl-6-(pyridin-2-yl)-7-phenyl-1a,2,3,7b-tetrahydro-1*H*-cyclopropa[*f*]-quinolin-3-yl]acetamide (**L**), which contains 2,2′-bipyridine and a moiety of the natural terpene (+)-3-carene, and investigate the properties of these complexes. The evaluation of cytotoxicity of the complexes is of particular interest. Copper complexes containing 2,2′-bipyridine molecules are known to exhibit a broad range of biological activities.[30,31]

Results and Discussion

The synthesis of the ligand **L** from the natural monoterpene hydrocarbon (+)-3-carene (**A**) is shown in Scheme 1.

Scheme 1

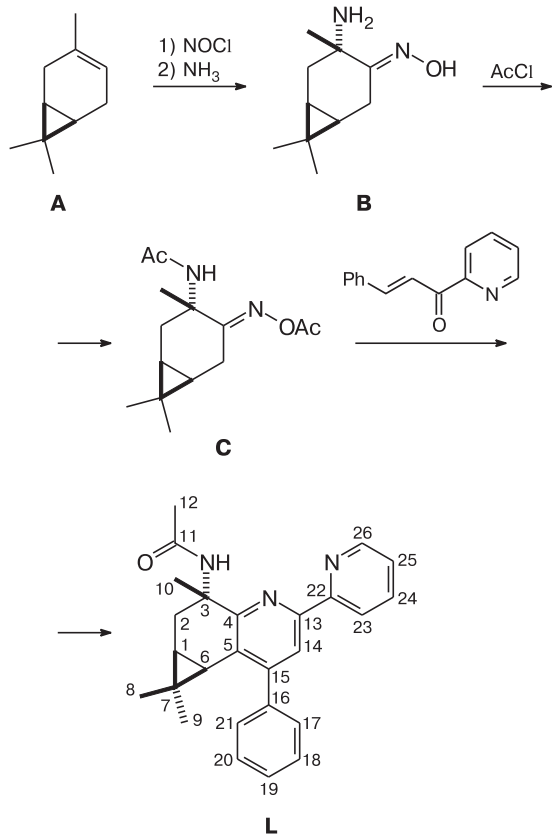

According to Scheme 1, (+)-3-carene (**A**) was treated with nitrosyl chloride to prepare nitroso chloride, and the reaction of the latter with excess aqueous ammonia gave α-amino oxime **B**. The treatment of the compound **B** with excess acetyl chloride afforded the *N*,*O*-diacetyl derivative **C**, which was used, without purification, in the condensation with (*E*)-3-phenyl-1-(pyridin-2-yl)prop-2-en-1-one synergistically catalyzed by CuI and diisopropylamine.[32] Finally, we obtained the compound **L** as a white powder in 26% yield based on the *N*,*O*-diacetyl derivative **C**. The chemical structure and the molecular configuration of the ligand **L** were confirmed by highly accurate analysis of NMR spectra.

The reaction of **L** with CuI in the $MeCN—CH_2Cl_2$ mixed solvent gave the compounds $\{[CuL_2][Cu_4I_6]\cdot MeCN\}_n$ (**1**) and $[Cu_4L_3I_4]\cdot 3\,MeCN$ (**2**), depending on the **L** : CuI ratio (1 : 1 and 1 : 2.5, respectively). These compounds differ in the composition and structure. Compound **1** is paramagnetic and has the magnetic moment μ_{eff} of 1.90 μ_B (300 K), which is close to the theoretical value (1.86 μ_B) for the Cu^{2+} ion, if the *g*-factor is 2.15. The invariance of μ_{eff} in the temperature range of 300—20 K attests to the absence of significant exchange interactions between Cu^{2+} ions (Fig. 1). Magnetochemical data indicate that compound **1** is a mixed-valence complex. When **L** : CuI = 1 : 1, Cu^{+} ions are partially oxidized to Cu^{2+}. When **L** : CuI = 1 : 2.5, the oxidation of Cu^{+} ions is not observed.

The crystal structure of mixed-valence complex salt **1** was determined by X-ray diffraction, which showed that this compound was composed of mononuclear complex cations $[Cu^{II}L_2]^{2+}$ (Fig. 2), polymeric polynuclear complex anions consisting of $(Cu^{I}_4I_6)^{2-}$ units, and MeCN molecules. The Cu(1) atom is coordinated by two N atoms and one O atom of one ligand **L** and by one N atom and one O atom of another ligand **L** (in Fig. 2, the atoms of the latter liagnd are labeled with the suffix A). Consequently, the ligands **L** and $\mathbf{L_A}$ show different coordination modes (tridentate and bidentate, respectively). The coordination gives rise to the polyhedron CuN_3O_2 (the coordination number (CN) of the Cu atom 5), which can be described as a distorted trigonal bipyramid with the Cu(1) N(2A)N(1)O(1A) equatorial plane (the rms deviation of the atoms from the plane is 0.023(1) Å). The apical vertices of the pyramid are occupied by the O(1) and N(2) atoms at distances of 1.951(3) and 1.901(3) Å, respectively, from the equatorial plane of the bipyramid. The Cu(1)—N bond lengths are somewhat different and are in the range

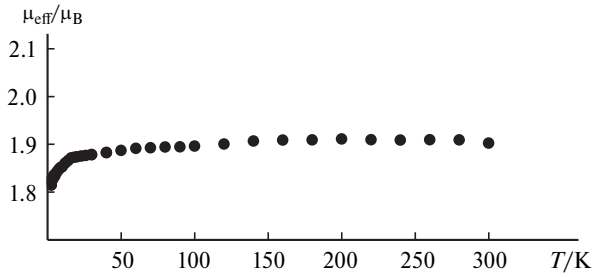

Fig. 1. Temperature dependence of μ_{eff} for compound **1**.

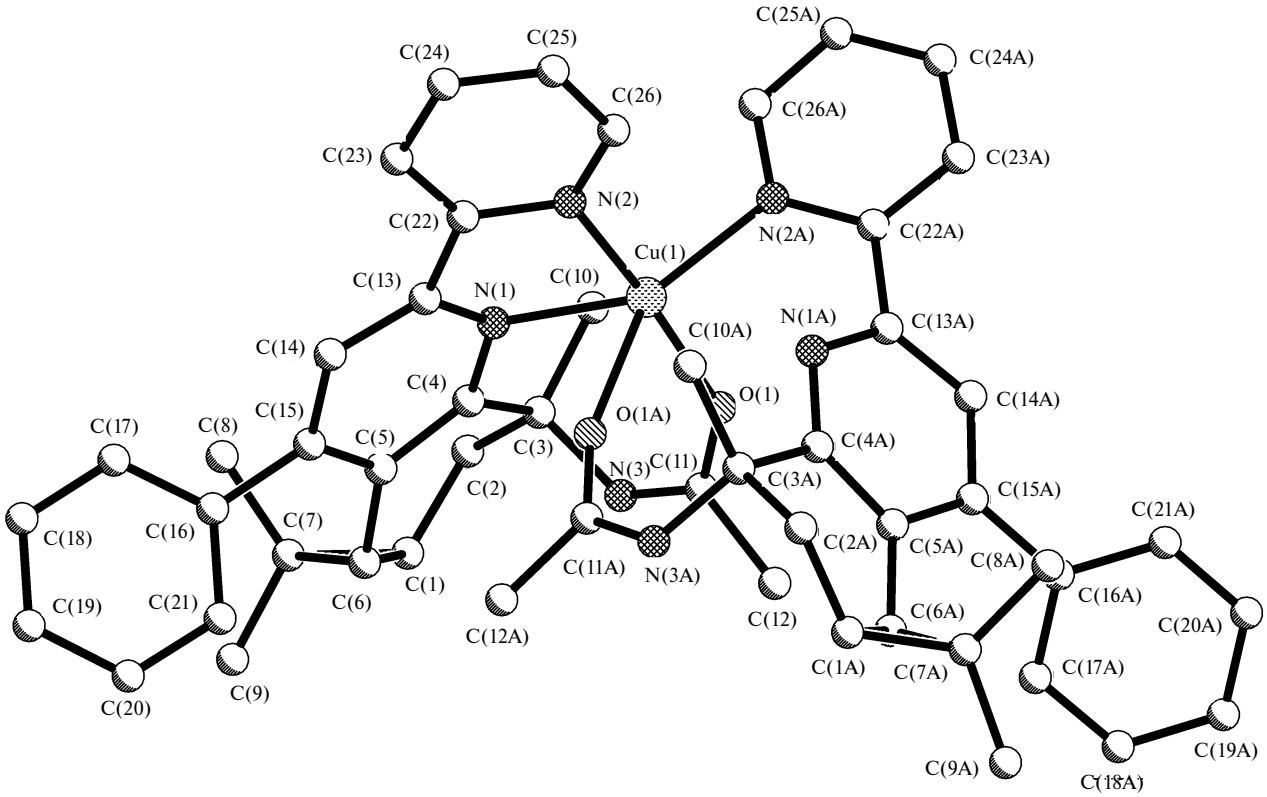

Fig. 2. Structure of the mononuclear complex cation $[Cu^{II}(L)_2]^{2+}$ of compound **1** and the atom numbering scheme.

of 1.956(4)—2.063(4) Å (Table 1). The Cu(1)—O(1) and Cu(1)—O(1A) distances are significantly different (1.942(3) and 2.305(4) Å, respectively). The coordination of the tridentate ligand **L** results in the closure of two chelate rings: the five-membered ring CuN_2C_2 adopting an envelope conformation (the N(1) atom deviates from the Cu(1)N(2)C(13)C(22) plane by 0.444(4) Å) and the seven-membered ring $CuNOC_3N$. As opposed to the ligand **L**, the coordination of the bidentate ligand $\mathbf{L_A}$ leads to the formation of the chelate ten-membered ring $CuNON_2C_5$. In this ring, the Cu(1)...N(1A) distance (2.770(4) Å) is substantially larger than the length of the Cu—N coordination bond. Therefore, the N(1A) atom of the ligand $\mathbf{L_A}$ is not included in the coordination sphere of the Cu(1) atom.

Apparently, the bidentate function of $\mathbf{L_A}$ is attributed to the steric effect due to the presence of bulky moieties in the ligands **L** and $\mathbf{L_A}$. In the molecules **L** and $\mathbf{L_A}$, the pyridine rings and phenyl groups are planar; the average deviations of the atoms from the planes are as follows: C(4)C(5)C(15)C(14)C(13)N(1), 0.038(2) Å; C(22)C(23)C(24)C(25)C(26)N(2), 0.005(3) Å; C(16)C(17)C(18)C(19)C(20)C(21), 0.007(3) Å; C(4A)C(5A)C(15A)C(14A)C(13A)N(1A), 0.026(2) Å; C(22A)C(23A)C(24A)C(25A)C(26A)N(2A), 0.007(3) Å; C(16A)C(17A)C(18A)C(19A)C(20A)C(21A), 0.006(3) Å. The six-membered carbocycles C(1)C(2)C(3)C(4)C(5)C(6) and C(1A)C(2A)C(3A)C(4A)C(5A)C(6A) adopt a distorted boat conformation. The deviations of the C(3) and C(6) atoms from the plane passing through the four carbon atoms C(1)C(2)C(4)C(5)

Table 1. Selected bond lengths (*d*) in the structures of compounds **1** and **2**

1		**2**	
Bond	*d*/Å	Bond	*d*/Å
Cu(1)—N(1)	2.063(4)	Cu(1)—N(1)	2.244(6)
Cu(1)—N(2)	1.956(4)	Cu(1)—N(2)	2.004(7)
Cu(1)—O(1)	1.942(3)	Cu(1)—I(1′)*	2.606(1)
Cu(1)—O(1A)	2.305(4)	Cu(1)—I(1)	2.621(1)
Cu(1)—N(2A)	2.023(4)	Cu(2)—I(2)	2.526(3)
N(1)—C(4)	1.345(6)	Cu(2)—I(1)	2.734(1)
N(1)—C(13)	1.343(4)	N(1)—C(13)	1.327(10)
N(2)—C(26)	1.343(6)	N(1)—C(4)	1.348(10)
N(2)—C(22)	1.348(4)	N(2)—C(26)	1.346(10)
N(3)—C(11)	1.326(5)	N(2)—C(22)	1.371(10)
N(3)—C(3)	1.480(4)	N(3)—C(3)	1.473(10)
N(1A)—C(4A)	1.341(6)	N(3)—C(11)	1.340(10)
N(1A)—C(13A)	1.334(6)	C(3)—C(10)	1.523(11)
N(2A)—C(22A)	1.346(6)	C(3)—C(2)	1.523(10)
N(2A)—C(26A)	1.339(6)	C(2)—C(1)	1.512(12)
N(1A)—C(13A)	1.334(4)	C(11)—O(1)	1.238(9)
N(3A)—C(3A)	1.478(6)	C(11)—C(12)	1.511(11)

* The symmetry code for the I(1′) atom: $1 - y$, $2 + x - y$, z.

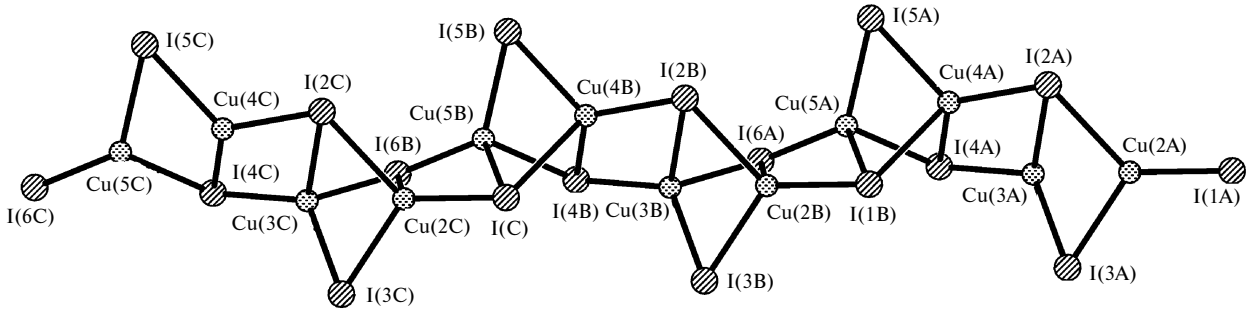

Fig. 3. Structure of the polymeric polynuclear complex anion consisting of $[Cu^{I}_4I_6]^{2-}$ units.

(Δ = 0.138(2) Å) are −0.571(5) and −0.161(5) Å, respectively; the deviations of the C(3a) and C(6a) atoms from the C(1A)C(2A)C(4A)C(5A) plane (Δ = 0.122(2) Å) are 0.632(6) and 0.184(6) Å. In the ligands **L** and $\mathbf{L_A}$, the dimethylcyclopropane ring, which is fused to the six-membered carbocycle through a common bond, forms dihedral angles of 124.7° and 124.3°, respectively. The pyridine rings are rotated about the C(13)—C(22) and C(13A)—C(22A) bonds by different angles. In the molecule **L**, this angle is 24.8°, whereas the corresponding angle in the molecule $\mathbf{L_A}$ is substantially larger (42.2°). The difference in the angles of rotation of one pyridine ring and the phenyl ring about the C(15)—C(16) and C(15A)—C(16A) lines is less significant (the corresponding angles are 59.5° and 54.1°).

The polynuclear complex anion composed of $(Cu_4I_6)^{2-}$ units has a polymeric structure (Fig. 3). In the anion, the Cu coordination polyhedra formed by four iodine atoms (CN 4) can be described as distorted tetrahedra. The bridging ligands — the I(1), I(2), I(4), and I(6) atoms — are coordinated to three Cu atoms, and the I(3) and I(5) atoms that are also bridging ligands are coordinated only to two Cu atoms. This coordination results in the formation of four-membered metallocycles Cu_2I_2 having a rhombic structure. The Cu_2I_2 rhombi share sides with CuI, resulting in the formation of polymeric zigzag ribbons. In the crystal structure, these ribbonds run parallel to each other along the *a* axis (Fig. 4). The Cu—I bond lengths in the metallocycles are different and depend on the number of bonds formed by the I atom with Cu atoms. In the rhombi involving the μ_3-ligands I(1), I(2), I(4), and I(6), the Cu—I bond lengths are considerably different (2.553(1)—3.107(1) Å). The bending of the metallocycles in these rhombi along the Cu...Cu line is insignificant (from 1.3° to 15.6°). The Cu(2)...Cu(5) and Cu(4)...Cu(5) distances are 2.671(2) and 2.691(3) Å, respectively. In the rhombi involving the μ-ligands I(3) and I(5), the Cu—I bonds are almost equal in length (2.624(1)—2.634(1) Å). These

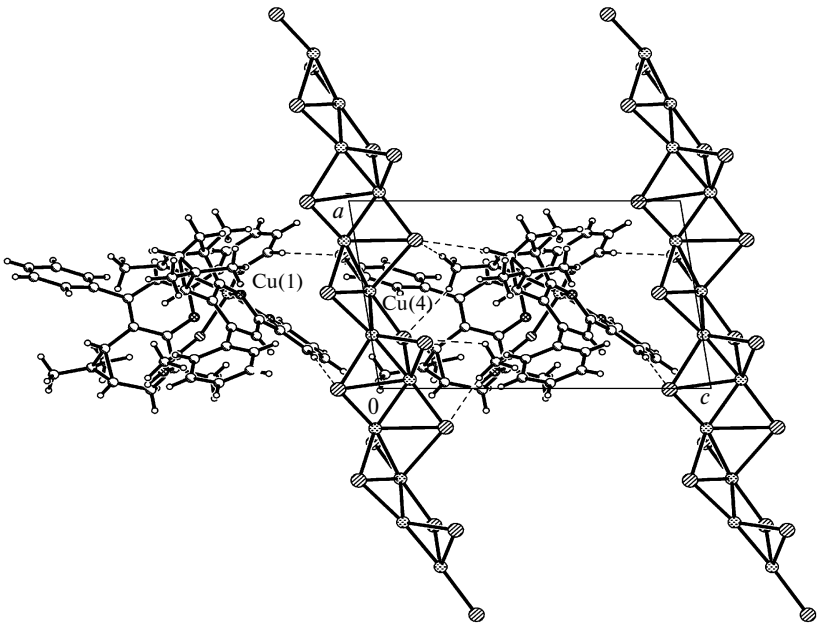

Fig. 4. Mutual arrangement of ions in the crystal structure of compound **1** projected onto the (010) plane.

metallocycles are significantly bent along the Cu...Cu line (120—133°). The Cu(2)...Cu(3) and Cu(4)...Cu(5) distances are 2.479(2) and 2.518(2) Å, respectively, and are substantially shorter than the Cu...Cu distances in the metallocycles containing iodide μ_3-ligands.

In the crystal structure, the $[Cu^{II}L_2]^{2+}$ cations are located between the parallel polymeric ribbons of anions. The shortest distance between the Cu atom of the complex cation and the Cu atom of the $(Cu^I{}_4I_6)^{2-}$ unit (Cu(1)...Cu(4)) is 6.154(2) Å (see Fig. 4). The cavities between the ribbons of anions and the cations are occupied by MeCN molecules (Fig. 5). The shortest distance between the C atoms of the MeCN molecule and the I atom of the complex anion (C(28)—H(28)...I(1), 3.820(4) Å) is consistent with van der Waals interactions, which suggests that compound **1** is a solvate.

The ionic complex Cu^I salts synthesized previously[33] are composed of complex cations, which are formed by Cs^+, K^+, Rb^+, and crown ether, and polymeric complex anions, the ribbons of which involve $(Cu^I{}_2I_3)^-$ units. In the metallocycles Cu_2I_2 of these compounds, the Cu...Cu distances are in the ranges of 2.430(9)—2.480(7) Å and 2.529(10)—2.697(6) Å, which are similar to the ranges of these distances in the metallocycles Cu_2I_2 in compound **1**. Besides, the synthesis of the salt $[(Me)_4N][Cu_2I_3]$ having two polymorphic forms (α and β) was reported.[34] In the α polymorph, the polymeric complex anion is a ribbon also consisting of $(Cu^I{}_2I_3)^-$ units. The anion contains metallocycles Cu_2I_2; the Cu...Cu distances are in the range of 2.34(2)—3.07(2) Å. In the structure of the complex $[(Me)_4N][Cu_2I_3]$, the Cu atoms are equally disordered over two positions. The Cu...Cu distance is significantly shorter (2.34(2) Å) than the corresponding distances in the polymeric ribbons in the structures of compound **1** (2.479(8) Å) and complexes,[33] in which the shortest Cu...Cu distance is 2.430(9) Å.

The crystal structure of compound **2** is composed of the tetranuclear Cu^I complex and MeCN molecules. The complex has a cubane-like molecular structure (Fig. 6). The vertices of the distorted cube lacking one vertex are occupied by Cu atoms and bridging I atoms. The Cu(1), Cu(1A), and Cu(1B) atoms are in general positions and are coordinated by two pyridine N atoms of the ligand **L** and two I atoms. The coordination of the bidentate ligand **L** results in the formation of the chelate ring CuN_2C_2. The Cu(1)—N bond lengths (Table 1) are substantially different (2.004(7) and 2.243(6) Å), whereas the Cu(1)—I bond lengths change only slightly (2.606(1) and 2.621 (1) Å). The Cu(2) atom occupies a special position on a three-fold axis. The coordination sphere of this copper atom is formed by four I atoms, three of which are bridging (Cu(2)—I, 2.734(1) Å) and one is terminal (Cu(2)—I, 2.526(3) Å) (see Table 1). The coordination polyhedra I_2N_2 and I_4 can be described as distorted tetrahedra (CN 4). Three four-membered square-planar metallocycles Cu_2I_2 form three faces of the cube; three Cu(1)...Cu(2) distances (diagonals

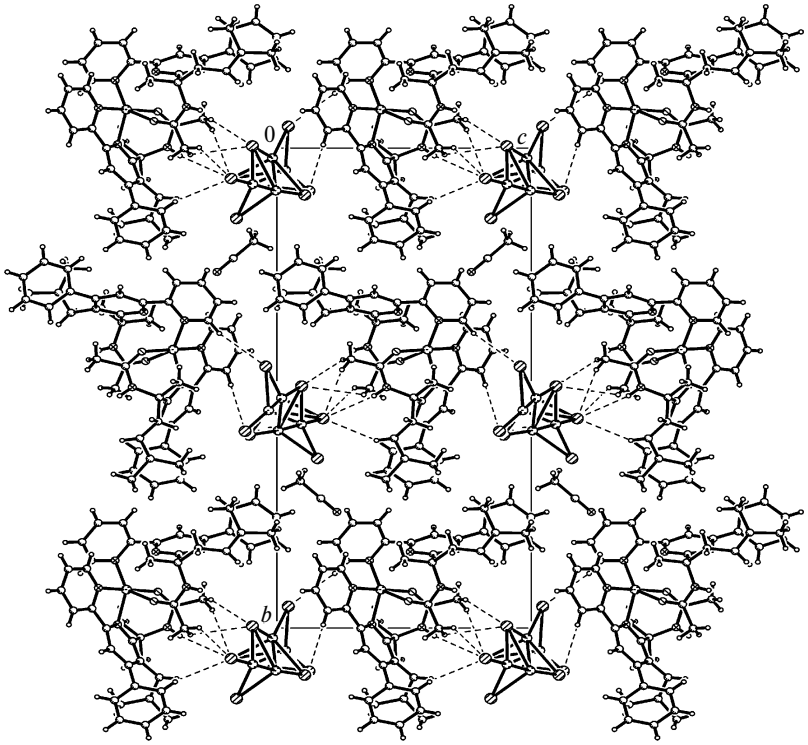

Fig. 5. Molecular packing in the crystal structure of solvate **1** projected onto the (100) plane.

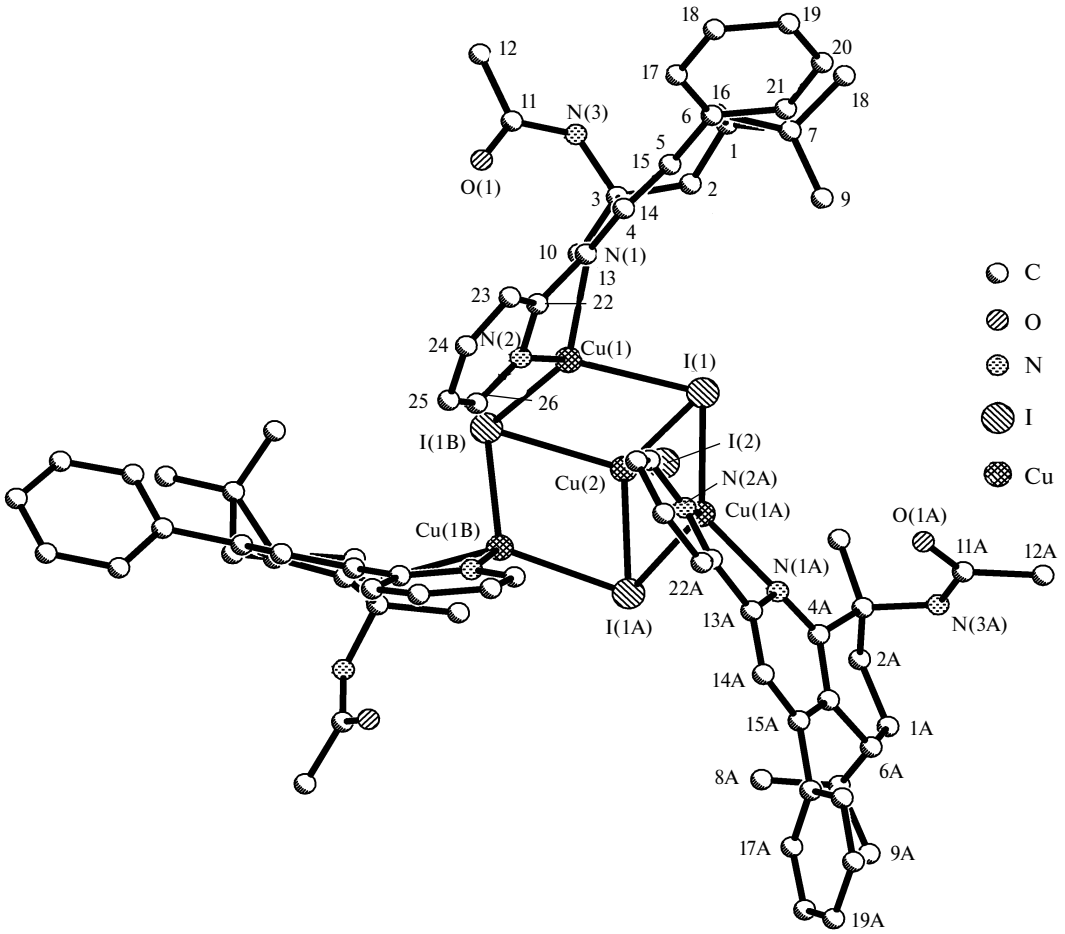

Fig. 6. Molecular structure of tetranuclear complex **2**.

of the square) are 3.178(2) Å. The Cu(1)...Cu(1A) and Cu(1)...Cu(1B) distances (4.014(3) Å) are much longer than the distances between the Cu atoms in the metallocycles.

The chelate ring adopts an envelope conformation with the Cu(1) atom deviating from the plane through the other four atoms of the ring by 0.578(9) Å. Both pyridine rings, N(1)C(4)C(5)C(15)C(14)C(13) and N(2)C(22)C(23)C(24)C(25)C(26), are nearly planar (the deviations are 0.031(4) and 0.007(4) Å, respectively); the bending angle along the C(13)—C(22) line is 22.2(2)°. The phenyl ring C(16)C(17)C(18)C(19)C(20)C(21) is planar; the deviation from the mean plane is 0.009(5) Å. The angle of rotation of the pyridine ring N(1)C(4)C(5)C(15)C(14)C(13) with respect to the phenyl ring about the C(15)—C(16) bond is 55.8(2)°. The six-membered carbocycle C(1)C(2)C(3)C(4)-C(5)C(6) adopts a distorted envelope conformation, with the C(3) atom deviating from the plane through the other five atoms of the carbocycle by 0.672(7) Å. The dimethylcyclopropane ring is fused to the six-membered carbocycle through the common C(1)—C(6) bond and forms a dihedral angle of 126.5(4)° with the plane through the five C atoms.

Figure 7 shows the molecular packing of complex **2** projected onto the (001) plane. In the crystal structure of **2**, discrete molecules of the complex are held together only by weak hydrogen bonds. The cavities between the molecules of the complex are occupied by MeCN molecules. The shortest I(1)...C(28) contact is 3.862(4) Å, which suggests that compound **2** is a solvate.

The influence of the ligand **L** and complex **2** on cell viability was evaluated using the Hep2 cell line (human laryngeal carcinoma) in the concentration range of 1—50 μmol L^{-1}. Cytotoxic activity was assessed by the double staining with the fluorescent dyes Hoechst 33342 and Propidium iodide, which provide the evaluation of the percentage of live, apoptotic, and dead cells.[35] The half-maximal inhibitory concentration (IC_{50}) was calculated as the concentration of the agent that causes 50% cell death.

The results of assays showed that both agents have pronounced cytotoxic activity and cause the dose-dependent response in cells (Fig. 8). The influence of the ligand **L** on the Hep2 cells becomes apparent at a concentration of 25 μmol L^{-1}. At this concentration, the percentage of apoptotic cells significantly increases (36%). At higher concentrations, the percentage of apoptotic cells reaches 62% (see Fig. 8, *a*). The IC_{50} value for the ligand is 30.5±0.5 μmol L^{-1}. Meanwhile, complex **2** exhibits cyto-

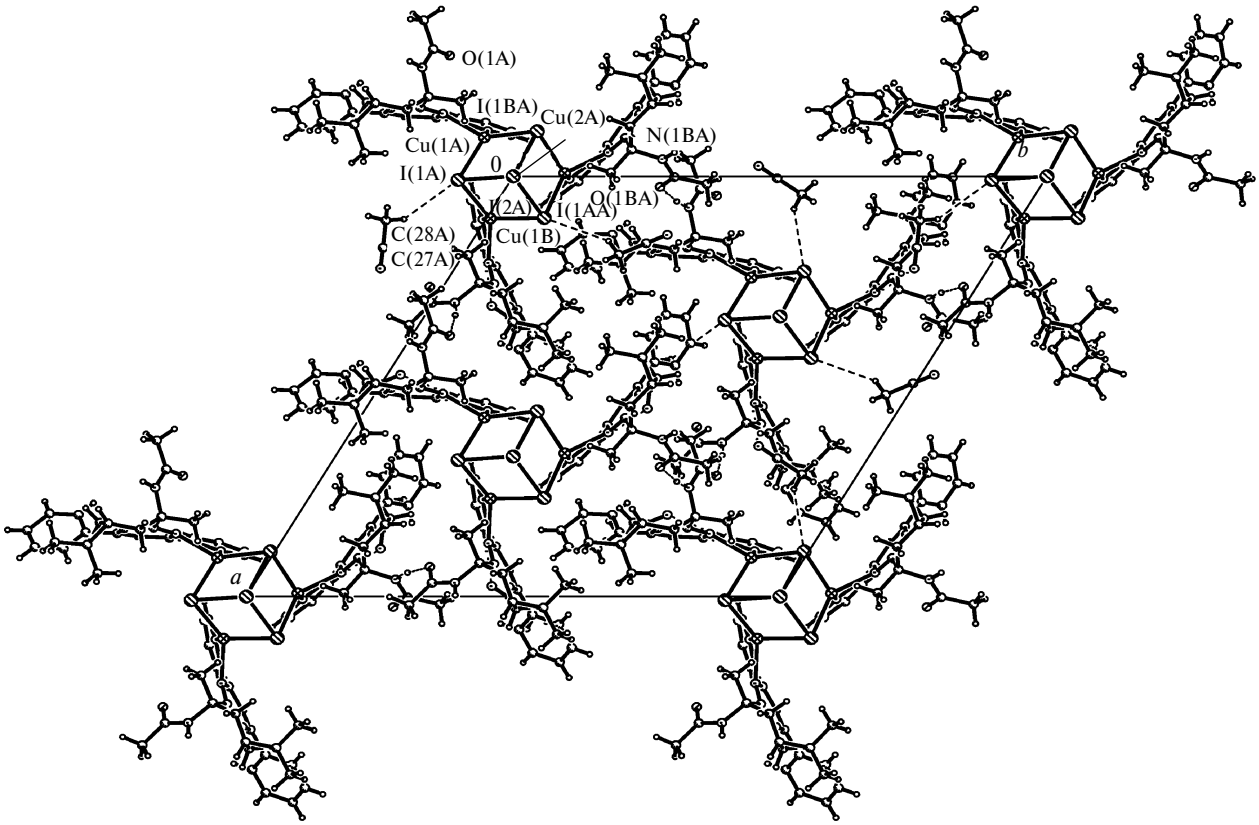

Fig. 7. Molecular packing in the crystal structure of compound **2** projected onto the (001) plane.

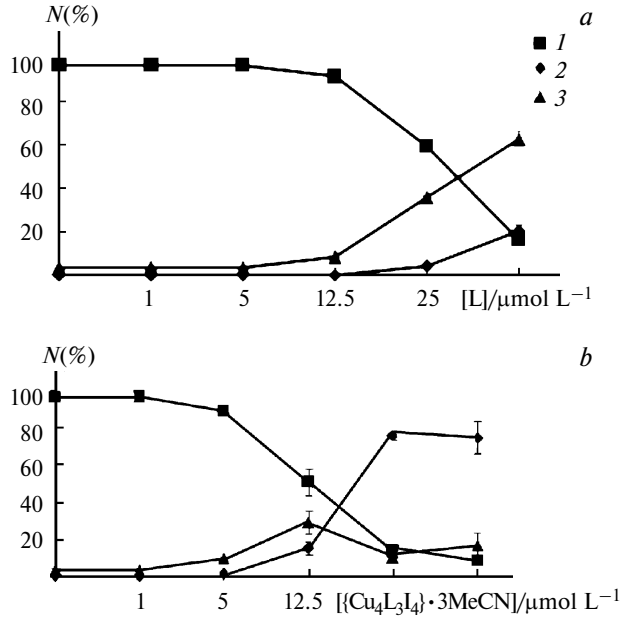

Fig. 8. Cytotoxic effect of compounds **L** (IC_{50} = 30.5±0.5 μmol L^{-1}) (*a*) and **2** (IC_{50} = 13.0±1.7 μmol L^{-1}) (*b*) on the Hep-2 cell line after exposure for 48 h: *1*, live cells; *2*, dead cells; *3*, apoptosis; *N* is the number of cells.

toxicity already at a concentration of 12.5 μmol L^{-1}, causing an increase in the percentage of apoptotic (30%) and dead (15%) cells; at a concentration of 25 μmol L^{-1}, up to 80% cells die (Fig. 8, *b*). Consequently, the complexation enhances cytotoxic activity observed for the free ligand, which is manifested as a more than a twofold decrease in IC_{50} for complex **2** (13.0±1.7 μmol L^{-1}) compared to that of the the free ligand **L** (30.5±0.5 μmol L^{-1}).

In summary, we synthesized copper iodide complexes with a chiral ligand — a 2,2′-bipyridine derivative containing the (+)-3-carene moiety. The X-ray diffraction study showed that mixed-valence complex **1** is a coordination polymer. Tetranuclear complex **2** has a cubane-like structure. An interesting structural feature of complex **2** is that the cube lacks one vertex. The evaluation of the influence of compounds **L** and **2** on viability of human laryngeal carcinoma cells (Hep2) showed that the complexation enhances cytotoxic activity observed for the free ligand.

Experimental

Reagents, solvents, and methods. The ligand **L** was synthesized using freshly distilled organic solvents (petroleum ether with b.p. 40—70 °C, ethyl acetate, dichloromethane, and ethanol (rectified 95%)), (+)-3-carene with b.p. 170—174 °C, n_D^{20} 1.4730,

$[\alpha]_D^{20}$ +16.0, which was obtained by the distillation of pine turpentine, sodium nitrite (analytical grade), 35% hydrochloric acid (reagent grade); 25% aqueous ammonia (analytical grade), acetyl chloride (high-purity grade), benzaldehyde (Reakhim, 99%), 2-acetylpyridine (Acros, 98%), NaOH (analytical grade), CuI (Reakhim, analytical grade), diisopropylamine (Acros, 99%), dimethyl sulfoxide (distilled *in vacuo* and stored over 4A molecular sieves), high-purity argon (TU 6-21-12-94), sodium tartrate dihydrate (Reakhim, analytical grade), and anhydrous sodium sulfate (analytical grade). The ligand **L** was purified by preparative adsorption column chromatography using silica gel with a mesh size of 50—160 μm (IMID); the separation was controlled by thin-layer chromatography on commercial Sorbfil plates (silica gel on polyamide film).

Nitrosyl chloride (NOCl) was prepared from sodium nitrite and hydrochloric acid and distilled before use. Dimeric crystalline nitrosyl chloride of (+)-3-carene was prepared by the reaction with NOCl in dichloromethane as described previously;[10] amino oxime **B** was synthesized from nitroso chloride by the reaction with excess aqueous ammonia in 95% ethanol.[36] (*E*)-3-Phenyl-1-(pyridin-2-yl)prop-2-en-1-one was prepared by the condensation of benzaldehyde with 2-acetylpyridine in the presence of NaOH in water at room temperature as described previously.[37] The complexes were synthesized using CuI (analytical grade), ethanol (rectified 95%), MeCN, CH_2Cl_2, and Pr^iOH (reagent grade).

Microanalyses for C, H, and N were carried out on an EuroEA 3000 analyzer. The temperature dependence of the magnetic susceptibility ($\chi(T)$) of compound **1** was measured on a Quantum Design MPM*SXL* SQUID magnetometer in the temperature range of 2—300 K at a magnetic field strength of 5 kOe. The paramagnetic components of the magnetic susceptibility of the complexes were evaluated taking into account the diamagnetic contribution estimated from the Pascal constants. The effective magnetic moment (μ_{eff}) was calculated by the equation $\mu_{eff} = [3k\chi T/(N_A\mu_B^2)]^{1/2}$, where N_A, μ_B, and k are Avogadro's number, the Bohr magneton, and the Boltzmann constant, respectively.

The NMR spectra were recorded on a Bruker DRX-500 spectrometer (^{1}H, 500.13 MHz; ^{13}C, 125.77 MHz) at 27 °C for solutions with a concentration of 25 mg mL^{-1} in a mixture of CCl_4 and $CDCl_3$ (1 : 1, v/v) using the signals of the solvent $CDCl_3$ (δ_C = 76.90, δ_H = 7.24) as the internal standard. The sign of the spin-spin coupling constants was not determined. The signal assignments were made based on ^{13}C NMR spectra recorded in the *J*-modulation mode (proton noise-decoupling, the opposite phases for signals of atoms with odd and even numbers of attached protons tuned to the constant J = 135 Hz), as well as on two-dimensional homonuclear ^{1}H—^{1}H correlation spectra, heteronuclear ^{13}C—^{1}H correlation spectra recorded for direct coupling constants (tuned to the constant J = 135 Hz), and heteronuclear ^{13}C—^{1}H correlation spectra recorded for long-range coupling constants (tuned to the constant J = 10 Hz). The ^{13}C—^{1}H spin-spin coupling constants were determined from the ^{13}C NMR spectra recorded in single resonance mode.

The cell viability was evaluated using an IN Cell Analyzer 2200 system (GE Healthcare, UK), which allows a high-throughput screening by a method described in the study.[35] The Hep2 cell line was cultured in 96-well plates containing IMDM culture medium, which were placed in a CO_2 incubator at 37 °C. After 24 h, compounds **L** and **2** dissolved in DMSO and acetone, respectively (the concentration range 1—50 μmol L^{-1}), were added and incubated for 48 h. Then the fluorescent dyes Hoechst 33342 and Propidium iodide were added. The cells were imaged using an IN Cell Analyzer 2200 system (GE Healthcare, UK) in an automatic mode for at least four fields per well. The images were processed with the In Cell Investigator software. The results are presented as the percentage of live, dead, and apoptotic cells from three independent experiments ± standard deviation.

***N*-{(1*S*,3*S*,6*R*,*E*)-4-Acetoxyimino-3,7,7-trimethylbicyclo-[4.1.0]heptan-3-yl}acetamide (C).** A solution of acetyl chloride (10.39 g, 0.1324 mol) in CH_2Cl_2 (20 mL) was added dropwise with stirring to a solution of amino oxime C (10.06 g, 0.0552 mol) and NEt_3 (13.37 g, 0.1321 mol) in CH_2Cl_2 (150 mL) under cooling in an ice bath. The reaction mixture was stirred with cooling for more 15 min, kept for 10 h at room temperature, and shaken with 1 *M* aqueous hydrochloric acid (20 mL). The organic phase was separated, washed with water until the wash water was neutral, dried with anhydrous Na_2SO_4, and concentrated *in vacuo*. The resulting *N,O*-diacetyl derivative was used in the synthesis without purification.

***N*-{(1a*S*,3*S*,7b*R*)-1,1,3-Trimethyl-7-phenyl-5-(pyridin-2-yl)-1a,2,3,7b-tetrahydro-1*H*-cyclopropa[*f*]quinolin-3-yl}acetamide (L).** A mixture of *N,O*-diacetyl derivative **C** (2.66 g, 10.0 mmol), diisopropylamine (2.02 g, 20.0 mmol), CuI (0.38 g, 2.0 mmol), and (*E*)-3-phenyl-1-(pyridin-2-yl)prop-2-en-1-one (2.51 g, 12.0 mmol) in DMSO (50 mL) was kept under an Ar atmosphere for 48 h at 80 °C, cooled to room temperature, and diluted with an aqueous ammonia solution (50 mL). Then sodium tartrate (0.1 g) was added, and the reaction products were extracted with EtOAc (3S15 mL). The combined organic extracts were dried with anhydrous Na_2SO_4 and concentrated *in vacuo*. The resulting dark oily product was chromatographed using the petroleum ether—EtOAc elution system (10 : 1 → 1 : 1, *v/v*). Ligand **L** was prepared in a yield of 1.033 g (26% based on *N,O*-diacetyl derivative **C**) as a fine white powder with m.p. 160—161 °C (from petroleum ether–EtOAc) and $[\alpha]^{27}_{589}$ +120 (*c* 0.30, $CHCl_3$). High-resolution EI-MS (70 eV). Found: *m/z* 397.2145 $[M]^+$. $C_{26}H_{27}O_1N_3$. Calculated: $[M]^+$ = 397.2149. EI-MS (70 eV), *m/z* (I_{rel} (%)): 397 $[M]^+$ (49), 339 $[M - CH_3CONH]^+$ (41), 338 $[M - CH_3CONH_2]^+$ (100), 337 (16), 323 $[M - CH_3CONH_2 - Me]^+$ (61), 181 (17), 169 (27), 149 (24), 131 (31), 119 (28), 69 (84). IR (KBr), ν/cm^{-1}: 3288 (N—H), 3050 (Ar—H), 1633 (C=O), 1537 (C=N). ^{1}H NMR ($CDCl_3$—CCl_4 1 : 1 *v/v*), δ: 0.69 (s, 3 H, H(8)); 0.94 (s, 3 H, H(9)); 1.21 (ddd, 1 H, H(1), J = 9.3 Hz, J = 8.5 Hz, J = 6.9 Hz); 1.40 (dd, 1 H, *pro-S*—H(2), J = 15.0 Hz, J = 6.9 Hz); 1.64 (d, 1 H, H(6), J = 8.5 Hz); 1.90 (s, 3 H, H(12)); 1.93 (s, 3 H, H(10)); 3.52 (dd, 1 H, *pro-R*-H(2), J = 15.0 Hz, J = 9.3 Hz); 5.37 (s, N—H); 7.23 (ddd, 1 H, H(25), J = 7.4 Hz, J = 4.8 Hz, J = 1.1 Hz); 7.35—7.44 (m, 5 H, H(17,18,19,20,21)); 7.77 (ddd, 1 H, H(24), J = 8.1 Hz, J = 7.4 Hz, J = 1.8 Hz); 8.31 (s, 1 H, H(14)); 8.48 (ddd, 1 H, H(23), J = 8.1 Hz, J = 1.1 Hz, J = 0.8 Hz); 8.58 (ddd, 1 H, H(26), J = 4.8 Hz, J = 1.8 Hz, J = 0.8 Hz). ^{13}C NMR ($CDCl_3$—CCl_4, 1 : 1 *v/v*,), δ: 16.16 (C(8), $^1J_{C,H}$ = 126 Hz); 20.18 (C(1), $^1J_{C,H}$ = 160 Hz); 23.31 (C(10), $^1J_{C,H}$ = 129) Hz); 24.54 (C(6), $^1J_{C,H}$ = 165 Hz); 24.55 (C(12), $^1J_{C,H}$ = 128 Hz); 25.05 (C(7)); 27.25 (C(9), $^1J_{C,H}$ = 126 Hz); 30.85 (C(2), $^1J_{C,H}$ = 132 Hz, $^1J_{C,H}$ = 128 Hz); 57.27 (C(3)); 120.80 (C(14), $^1J_{C,H}$ = 165 Hz, $^{2,3}J_{C,H}$ < 0.3 Hz); 121.04 (C(23), $^1J_{C,H}$ = 166 Hz, $^{2,3}J_{C,H}$ = 6.5 Hz); 123.35 (C(25), $^1J_{C,H}$ = 164 Hz, $^{2,3}J_{C,H}$ = 8.3 Hz, $^{2,3}J_{C,H}$ = 6.5 Hz); 127.90 (C(19), $^1J_{C,H}$ = 160 Hz, $^{2,3}J_{C,H}$ = 7.1 Hz, $^{2,3}J_{C,H}$ = 7.1 Hz); 128.00 (C(17), C(21), $^1J_{C,H}$ = 160 Hz, $^{2,3}J_{C,H}$ = 6.8 Hz); 128.75 (C(18), C(20), $^1J_{C,H}$ = 159 Hz, $^{2,3}J_{C,H}$ = 6.3 Hz, $^{2,3}J_{C,H}$ = 6.3 Hz); 129.55

(C(5), $^{2,3}J_{C,H}$ = 6.2 Hz, $^{2,3}J_{C,H}$ = 2.7 Hz); 136.57 (C(24), $^{1}J_{C,H}$ = 162 Hz, $^{2,3}J_{C,H}$ = 6.7 Hz); 139.49 (C(16)), 148.91 (C(26), $^{1}J_{C,H}$ = 178 Hz, $^{2,3}J_{C,H}$ = 7.0 Hz, $^{2,3}J_{C,H}$ = 3.4 Hz); 152.21 (C(13)); 152.45 (C(15)); 156.20 (C(22)); 159.85 (C(4)); 168.95 (C(11)).

Preparation of single crystals of compound {[CuL_2]-[Cu_4I_6] · MeCN}$_n$ (1). A solution of CuI (0.010 g, 0.05 mmol) in MeCN (2.5 mL) was added with stirring to a solution of ligand **L** (0.020 g, 0.05 mmol) in a mixture of MeCN (2.5 mL) and CH_2Cl_2 (2 mL). The beaker containing the orange solution was covered with a perforated paraffin film sheet and allowed to stand at room temperature until the solvent was completely evaporated. A single crystal suitable for X-ray diffraction was selected from intergrowths of dark-green needle-like crystals. Besides, crystals were taken for elemental analysis and magnetochemical measurements. Found (%): C, 34.0; H, 3.0; N, 5.1. $C_{54}H_{57}N_7O_2Cu_5I_6$. Calculated (%): C, 33.9; H, 3.0; N, 5.1.

Synthesis of compound [$Cu_4L_3I_4$] · 3MeCN (2). A solution of CuI (0.048 g, 0.25 mmol) in MeCN (4 mL) was added with stirring to a solution of free ligand **L** (0.040 g, 0.1 mmol) in a MeCN—CH_2Cl_2 mixture (1 : 1, v/v; 4 mL). The beaker containing the orange solution was covered with a watch glass and allowed to stand for 16 h at room temperature, thus causing the formation of intergrowths of orange crystals. The reaction mixture was kept for 7 days, after which single crystals formed. Single crystals for X-ray diffraction were selected from the mixture, and the remaining crystals were filtered off and washed with Pr^iOH. The yield 0.056 g (80%). Found (%): C, 49.6; H, 4.5; N, 7.8. $C_{84}H_{90}N_{12}O_3Cu_4I_4$. Calculated (%): C, 48.6; H, 4.4; N, 8.1.

X-ray diffraction study. A green crystal of compound **1** and an orange crystal of complex **2** were selected for X-ray diffraction study. The unit cell parameter were determined and the reflection intensities were measured on an X8 APEX automated diffractometer by a standard procedure at 150 K (Mo-Kα, graphite monochromator, α-scanning technique with a step of 0.5°). Principal crystallographic characteristics and the X-ray diffraction data and structure refinement statistics for complexes **1** and **2** are given in Table 2. Acentric space groups for the crystal structures of the complexes were chosen based on the analysis of systematic absences and were supported by calculations. The structures were solved by direct methods with the SHELX-2014 program package[38] and were refined by the full-matrix least-squares with anisotropic displacement parameters for all nonhydrogen atoms. The hydrogen atoms were positioned geometrically and refined isotropically together with nonhydrogen atoms. Difference electron density ρ(*xyz*) maps calculated in the course of the refinement revealed, apart from the identified peaks, additional peaks interpreted as atoms of MeCN molecules in the crystal structures of compounds **1** and **2**. Selected interatomic

Table 2. Crystallographic characteristics and the X-ray diffraction data collection and structure refinement statistics for compounds **1** and **2**

Parameter	**1**	**2**
Molecular formula	$C_{54}H_{57}Cu_5I_6N_7O_2$	$C_{84}H_{90}Cu_4I_4N_{12}O_3$
Molecular weight	1915.17	2077.43
Crystal system	Monoclinic	Trigonal
Space group	$P2_1$	$R3$
a/Å	8.3488(4)	23.9718(6)
b/Å	27.743(2)	23.9718(6)
c/Å	12.8970(7)	12.3463(6)
α/deg	—	90.0
β/deg	98.257(2)	90.0
γ/deg	—	120.0
V/Å^3	2956.3(3)	6144.2(4)
Z	2	3
d_{calc}/g cm^{-3}	2.151	1.684
μ/mm^{-1}	4.948	2.588
Crystal size/mm	0.24×0.1×0.09	0.21×0.18×0.12
θ-Scanning range/deg	1.60—32.72	1.70—27.49
Number of reflections		
measured	40500	14340
unique	18231	6112
R_{int}	0.0251	0.0432
with $I > 2\sigma(I)$	17008	5174
Number of refined parameters	676	327
GOOF on F^2	1.017	1.032
R-factor, $I > 2\sigma(I)$		
R_1	0.0292	0.0381
wR_2	0.0593	0.0843
R-factor (based on all I_{hkl})		
R_1	0.0329	0.0525
wR_2	0.0607	0.0892
Residual electron density, (ρ_{max}/ρ_{min})/e Å^{-3}	2.10/−1.68	1.04/−1.41
Flack parameter	0.006(5)	0.030(12)

Table 3. Selected bond angles (ω) in the structures of compounds **1** and **2**

Bond	ω/deg
1	
N(1)—Cu(1)—N(2)	81.5(2)
N(2)—Cu(1)—N(2A)	94.8(2)
N(2A)—Cu(1)—O(1A)	139.8(2)
N(2A)—Cu(1)—N(1)	141.2(2)
O(1)—Cu(1)—O(1A)	85.9(2)
O(1)—Cu(1)—N(1)	98.8(2)
O(1)—Cu(1)—N(2)	171.7(2)
O(1)—Cu(1)—N(2A)	90.1(2)
N(1)—Cu(1)—O(1A)	78.8(2)
N(2)—Cu(1)—O(1A)	86.0(2)
2	
N(1)—Cu(1)—N(2)	78.6(3)
N(1—Cu(1)—I(1′)	140.0(1)
N(2)—Cu(1)—I(1′)	107.7(2)
N(2)—Cu(1)—I(1)	123.1(2)
N(1)—Cu(1)—I(1)	96.6(2)
I(1′)—Cu(1)—I(1)	110.6(1)
I(1)—Cu(2)—I(1′)	103.6(1)
Cu(1′)—I(1)—Cu(1)	100.3(1)
Cu(1)—I(1)—Cu(2)	72.8(1)

distances and bond angles are given in Tables 1 and 3, respectively. Complete tables of atomic coordinates, bond lengths, and bond angles were deposited with the Cambridge Crystallographic Data Centre (CCDC 1811910 and 1811911) and can be obtained from the authors.

The study was performed using equipment of the Joint Access Center "Proteomic analysis" of the Institute of Molecular Biology and Biophysics (IMBB).

This study was financially supported by the Russian Foundation for Basic Research and the Government of the Novosibirsk region (Project No. 17-43-540857 r_a).

References

1. S. Sharma, M. Chauhan, A. Jamsheera, S. Tabassum, F. Arijmand, *Inorg. Chim. Acta*, 2017, **458**, 8.
2. G. Muller, *Dalton Trans.*, 2009, 9692.
3. T. Wu, X.-Z. You, P. Boun, *Coord. Chem. Rev.*, 2015, **284**, 1.
4. J. Grassous, *Chem. Soc. Rev.*, 2009, **38**, No 3, 830.
5. R. Carr, N.H. Evans, D. Parcer, *Chem. Soc. Rev.*, 2012, **41**, 7673.
6. K. Inoue, Sh.-I. Ohkoshi, H. Imai, *Magnetism: Molecules to Materials V*, Eds J. S. Miller, M. Drillon, Wiley-VCH VerlagGmbH, Weinheim (FRG), 2002, 42.
7. X.-L. Li, K. Chen, Y. Liu, Z.-X. Wang, T.-W. Wang, J.-L. Zuo, Y.-Z. Li, Y. Wang, J. S. Zhu, J.-M. Liu, Y. Song, X.-Z. You, *Angew. Chem., Int. Ed.,* 2007, **46**, 6820.
8. A. von Zelewsky, O. Mamula, *J. Chem. Soc.*, *Dalton Trans.*, 2000, 219.
9. O. Mamula, A. von Zelewsky, *Coord. Chem. Rev.*, 2003, **242**, 87.
10. A. V. Tkachev, *Mendeleev Chem. J.*, 1998, **42**, 42.
11. S. V. Larionov, A. V. Tkachev, *Mendeleev Chem. J.*, 2004, **48**, 154.
12. S. V. Larionov, *Russ. J. Coord. Chem.*, 2012, **38**, 1.
13. G. Muller, J.-C. G. Bünzli, J. P. Riehl, D. Suhr, A. von Zelewsky, H. Mürner, *Chem. Commun.*, 2002, 1522.
14. J. L. Lunkley, D. Shirotani, K. Yamanari, S. Kaizaki, G. Muller, *Inorg. Chem.*, 2011, **50**, 12724.
15. K. D. Oyler, F. J. Coughlin, S. Bernhard, *J. Am. Chem. Soc.*, 2007, **129**, 210.
16. S. V. Larionov, Z. A. Savel'eva, R. F. Klevtsova, L. A. Glinskaya, E. M. Uskov, S. A. Popov, A. V. Tkachev, *Russ. J. Struct. Chem.*, 2010, **51**, 519.
17. S. V. Larionov, Z. A. Savel'eva, R. F. Klevtsova, L. A. Glinskaya, E. M. Uskov, M. I. Rakhmanova, S. A. Popov, A. V. Tkachev, *Russ. J. Struct. Chem.*, 2011, **52**, 531.
18. T. E. Kokina, L. A. Glinskaya, A. V. Tkachev, V. F. Plyusnin, Yu. V. Tsoy, I. Yu. Bagryanskaya, E. S. Vasilyev, D. A. Piryazev, L. A. Sheludyakova, S. V. Larionov, *Polyhedron*, 2016, **117**, 437.
19. T. E. Kokina, L. A. Glinskaya, E. S. Vasiliev, M. I. Rakhmanova, S. V. Makarova, D. A. Piryazev, I. V. Korol´kov, A. V. Tkachev, S. V. Larionov, *Russ. J. Struct. Chem.*, 2017, **58**, 1027.
20. C. Duncan, A. R. White, *Metallomics*, 2012, **4**, 127.
21. C. Santini, M. Pelei, V. Gandin, M. Porchia, F. Tisato, C. Marzano, *Chem. Rev.*, 2014, **114**, 815.
22. D. Krajčiová, M. Melník, E. Havránek, A. Forgácsová, P. Mikuś, *J. Coord. Chem.*, 2014, **67**, 1493.
23. M. Wehbe, A. W. Y. Leung, M. J. Abrams, C. Orvig, M. B. Bally, *Dalton Trans.*, 2017, **46**, 10758.
24. P. Jia, R. Ouyang, P. Cao, X. Tong, X. Zhou, T. Lei, Yu. Zhao, N. Guo, H. Chang, Yu. Miao, Sh. Zhou, *J. Coord. Chem.*, 2017, **70**, 2175.
25. T. A. Fernandes, F. Mendes, A. P. S. Roseiro, I. Santos, M. F. N. N. Carvalho, *Polyhedron*, 2015, **87**, 215.
26. M. E. S. Serra, D. Murtinho, Z. N. da Rocha, A. S. Pires, J. G. Baptista, A. M. Abrantes, M. Laranjo, J. E. Casalta-Lopes, M. F. Botelho, A. A. C. C. Pais, S. C.C. Nunes, H. D. Burrows, T. Costa, *Polyhedron*, 2017, **137**, 147.
27. B.-L. Fei, Z.-X. Huang, W.-Sh. Xu, D.-D. Li, Ya. Lu, W.-L. Gao, Yu. Zhao, Yu Zhang, Q.-B. Liu, *J. Photochemistry Photobiology, B: Biology*, 2016, **160**, 43.
28. N. Armaroli, G. Accorsi, F. Cardinali, A. Listorti, *Top. Curr. Chem.*, 2007, **280**, 69.
29. P. Ford, E. Cariarti, J. Bourassa, *Chem. Rev.*, 1999, **99**, 3625.
30. C. Marzano, M. Pellei, F. Tisato, C. Santini, *Anti-Cancer Agents in Medicinal Chemistry*, 2009, **9**, 185.
31. R. Galindo-Murillo, J. C. Garcia-Ramos, L. Ruiz-Azuara, T. E. Cheatham, F. Cortés-Guzmán, *Nucleic Acids Res.*, 2015, **43**, 5364.
32. Y. Wei, N. Yoshikai, *J. Am. Chem. Soc.*, 2013, **135**, 3756.
33. A. Nurtaeva, E. M. Holt, *Acta Cryst.*, 1998, **C54**, 594.
34. S.-L. Li, R. Zhang, J.-J. Hou, X.-M. Zhang, *Inorg. Chem. Commun.*, 2013, **32**, 12.
35. A. V. Artem´ev, J. A. Eremina, E. V. Lider, O. V. Antonova, E. V. Vorontsova, I. Yu. Bagryanskaya, *Polyhedron*, 2017, **138**, 218.
36. P. A. Petukhov, A. V. Tkachev, *Tetrahedron,* 1997, **53**, 2535.
37. V. V. Zakharychev, A. V. Kuzenkov, *Chem. Heterocycl. Compd.*, 2007, **43**, 989.
38. G. M. Sheldrick, *Acta Crystallogr. Sect. C: Cryst. Struct. Commun.*, 2015, **71**, 3.

Received December 22, 2017;
in revised form April 25, 2018;
accepted May 4, 2018